Department of Physics and Astronomy
University of Heidelberg

Bachelor Thesis in Physics
submitted by

Felix Friedrich Florian Frey

born in Kirchheim unter Teck (Germany)

2012

Particle Production in Ultra-Relativistic Heavy-Ion Collisions and the Constituent Participant Model

This Bachelor Thesis has been carried out by Felix Frey at the
Physikalisches Institut in Heidelberg
under the supervision of
PD Dr. Klaus Reygers

Abstract

Multiplicity measurements in high-energy heavy-ion collisions are performed to get a better understanding of the particle production process. For the nucleon participant model one has shown that it fails in the description of heavy-ion collisions. Within this thesis we demonstrate that the charged particle multiplicity in heavy-ion collisions can be described with a constituent participant model.

We show that the centrality dependence of the charged particle multiplicity at midrapidity in Au+Au collisions at $\sqrt{s_{NN}} = 200\,\text{GeV}$ is proportional to the number of participating constituent quarks. However, it is shown that this does not hold for the total charged multiplicity (integrated over pseudorapidity η).

Additionally we demonstrate that the total charged multiplicity can be better described within a diquark model. In the diquark model the total charged multiplicity scales consistently with the number of participating constituents from p+p and d+Au to Au+Au.

Kurzdarstellung

Multiplizitätsmessungen in hochenergetischen Schwerionenkollisionen werden gemacht, um ein besseres Verständnis des Teilchenproduktionsprozesses zu erlangen. Für das Nucleon-Participant-Modell konnte gezeigt werden, dass es die Teilchenproduktion in Schwerionenkollisionen nicht beschreiben kann. Diese Arbeit zeigt, dass die Multiplizität in Schwerionenkollisionen innerhalb eines Konstituenten-Quark Modells beschrieben werden kann.

Es wird gezeigt, dass die zentralitätsabhängige Multiplizität bei mittlerer Rapidität in Au+Au-Kollisionen bei einer Schwerpunktsenergie von $\sqrt{s_{NN}} = 200\,\text{GeV}$ proportional zur Anzahl der teilnehmenden Konstituenten-Quarks ist. Bei Au+Au Kollisionen mit gleicher Schwerpunktsenergie ist die gesamte Multiplizität hingegen nicht mit der Anzahl der teilnehmenden Quark-Konstituenten skalierbar.

Außerdem zeigen wir, dass sich die gesamte Multiplizität besser mit der Anzahl der teilnehmenden Quark-Konstituenten innerhalb eines Diquark-Modells beschreiben lässt. Im Diquark-Modell skaliert die gesamte Multiplizität konsistent von p+p und d+Au bis zu Au+Au-Kollisionen mit der Anzahl der teilnehmenden Quark-Konstituenten.

Contents

1 Introduction

Particle production in ultra-relativistic heavy-ion collisions belongs to the subjects in high-energy physics which are of particular interest in current research [Arm09, Col11a].

Thousands of particles are created in ultra-relativistic heavy-ion collisions, when two nuclei collide head-on. Particle production processes are typically characterized as either soft or hard which means that the transferred momentum is either below or above 1-2 GeV. There are several models and different theories aiming to describe the produced multiplicity (the number of produced particles) in such collisions. One idea is to assume that in collisions where hard processes can be neglected the relevant sources for particle production are colliding constituent quarks. If so, the produced multiplicity can be described in a constituent participant model in which the multiplicity scales with the number of quark participants (Q_{part}). The number of quark participants can be computed in Glauber-Monte-Carlo simulations. This approach is studied in this thesis.

In the following the steps between the idea of quark participant scaling and the results of the constituent participant model are explained.

In Section 2 the basic idea of the constituent participant model is explained. At first the idea to scale the multiplicity in p+A (proton-ion) collisions with the number of nucleon participants (N_{part}) is recapitulated. Then the concept of quark participants is developed.

In Section 3 the most important equations and terms as well as the Glauber model are introduced. In addition we discuss the diquark model, which is also applied to describe the multiplicity in A+A collisions. Furthermore a theoretical motivation is given why it is reasonable to describe particle production within the constituent participant model.

In Section 4 the methods and techniques used to simulate heavy-ion collisions within Glauber-Monte-Carlo simulations are described and explained.

In Section 5 we present and discuss the results. The constituent participant model in which nucleons are composed of three constituent quarks as well as the diquark model in which nucleons are composed of a quark and a diquark are studied.

A summary of all results as well as a short outlook is given in Section 6.

1

2 Particle Production in Ultra-Relativistic Heavy-Ion Collisions

In ultra-relativistic heavy-ion physics, heavy-ion collisions are explored in an energy regime where the rest energy is negligible in comparison with the kinetic energy of the interacting ions. In case of a heavy-ion collision where the available energy exceeds the threshold energy for particle production, new particles are created ($\sqrt{s_{\mathrm{NN}}} \geq m_{\mathrm{p}}$, where $\sqrt{s_{\mathrm{NN}}}$ is the center-of-mass energy per nucleon pair and m_{p} is the mass of a created particle). To explain these particle production processes different models and theories are applied. One can distinguish between particle production in either soft processes where the transferred momentum is below 1-2 GeV (and therefore the energy is on the order of the mass $E \approx m$) or hard processes where the transferred momentum is above 1-2 GeV ($E \gg m$)[Won94, KDW05].

In soft processes particles can be modeled as the fragmentation of color flux tubes ("strings") stretched between constituent quarks of colliding particles. String fragmentation corresponds to the formation of quark-antiquark pairs. The multiplicity in soft processes is approximately proportional to the number of nucleon participants. More precisely: Participants are nucleons which have suffered at least one inelastic collision (N_{part}, see Section 3.1).

In hard processes there are bunches of colliding quarks and gluons that interact. After getting scattered, they fragment via the strong interaction into jets of new particles. The multiplicity in hard processes is proportional to the number of nucleon collisions (N_{coll}, see Section 3.1).

In the constituent participant model the multiplicity in heavy-ion collisions is described by the number of quark constituents. The model is introduced in the following.

2.1 The Nucleon Participant Model and Particle Production in p+A Collisions

The initial idea of the constituent participant model is the observation that the multiplicity in p+A collisions can be described with the number of nucleon participants. [BHL$^+$80].

$$\frac{\langle N_{p+A} \rangle}{\langle N_{p+p} \rangle} \approx \frac{1 + N_{\text{coll}}}{2}$$
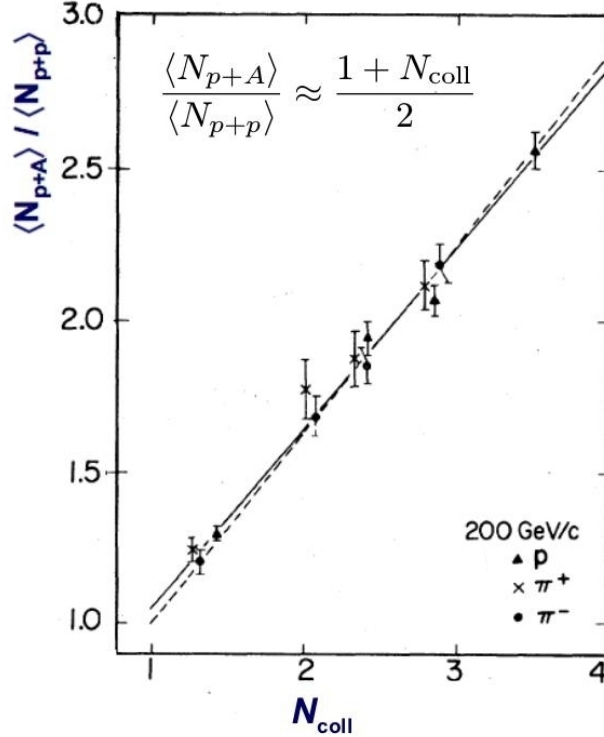
Figure 1: The ratio of averaged multiplicity in p+A collisions $\langle N_{\text{p+A}} \rangle$ to averaged multiplicity in p+p collisions $\langle N_{\text{p+p}} \rangle$ at $\sqrt{s_{\text{NN}}} = 200\,\text{GeV}$ is plotted versus the number of nucleon collisions N_{coll}. We see that nucleon participants describe the scaling. Plot taken from [BHL$^+$80]. The labels of the axes are modified.

For p+A collisions the simple relation $N_{\text{part}} = N_{\text{Coll}} + 1$ holds. For instance, if a proton collides with a nucleus composed of three nucleons and the proton hits every nucleon, there are three collisions and four participants. We see in Figure 1 that the ratio of produced particles does not scale with the number of nucleon collisions, but approximately with the number of nucleon participants. Hence, the multiplicity in p+A collisions is approximately proportional to the number of nucleon participants.

2.2 The Nucleon Participant Model and Particle Production in A+A Collisions

The next step is to apply the nucleon participant model to A+A (ion-ion) collisions [Col11a]. This is shown in Figure 2.
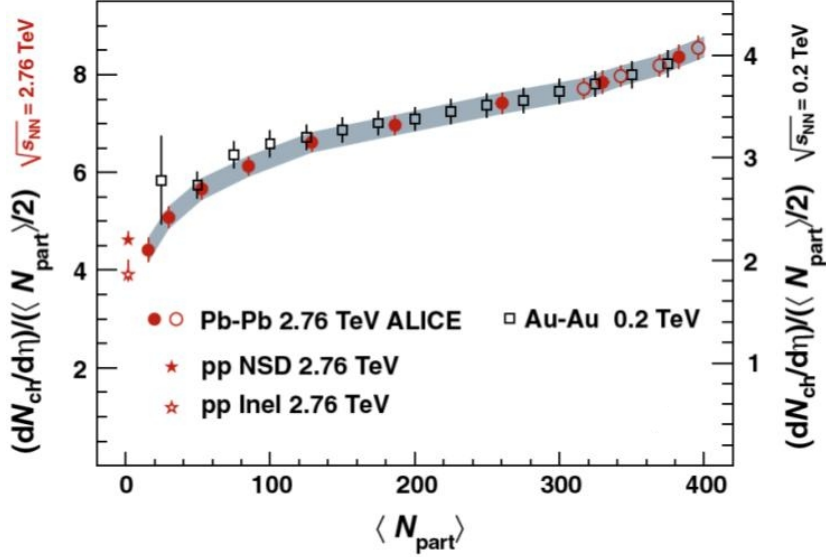
Figure 2: The ratio of charged particle multiplicity per pseudorapidity unit at midrapidity $dN_{ch}/d\eta$ (see, Section 3.2) to the number of nucleon participant pairs $\langle N_{part}\rangle/2$ is plotted at a center-of-mass energy of $\sqrt{s_{NN}} = 2.76\,\text{TeV}$ (LHC-energy, Pb+Pb (lead-lead) collisions) versus $\langle N_{part}\rangle$ as solid circles . The same ratio but for an energy of $\sqrt{s_{NN}} = 200\,\text{GeV}$ (RHIC-energy, Au+Au (gold-gold) collisions) is plotted as open squares. The measured multiplicity is not proportional to the number of nucleon participant pairs. Plot taken from [Col11a].

From Figure 2 it is obvious that the number of produced particles does not scale with the number of nucleon participants for $\sqrt{s_{NN}} = 200\,\text{GeV}$ and $\sqrt{s_{NN}} = 2.76\,\text{TeV}$, respectively. (at $\sqrt{s_{NN}} = 200\,\text{GeV}$ measurements were performed at the Relativistic Heavy Ion Collider (RHIC), whereas at $\sqrt{s_{NN}} = 2.76\,\text{TeV}$ measurements were performed at the Large Hadron Collider (LHC), see Section 4.5.) Otherwise the ratio would not change by increasing the number of participants, a quantity that describes the centrality of a collision (see Section 3.4).
Nevertheless the shape of the yield per participant pair is at RHIC and LHC quite similar. Therefore one concludes that there is a similarity in the production mechanism for the multiplicity at $\sqrt{s_{NN}} = 200\,\text{GeV}$ and $\sqrt{s_{NN}} = 2.76\,\text{TeV}$.

2.3 The Constituent Participant Model and Particle Production in A+A Collisions

A simple idea to explain the similarity in the production mechanism is to assume that each nucleon consists of 3 constituent quarks. The concept of the constituent participant model is explained in [ASS78, HL82] and references therein. For RHIC data this is studied in Figure 3 [EV03].
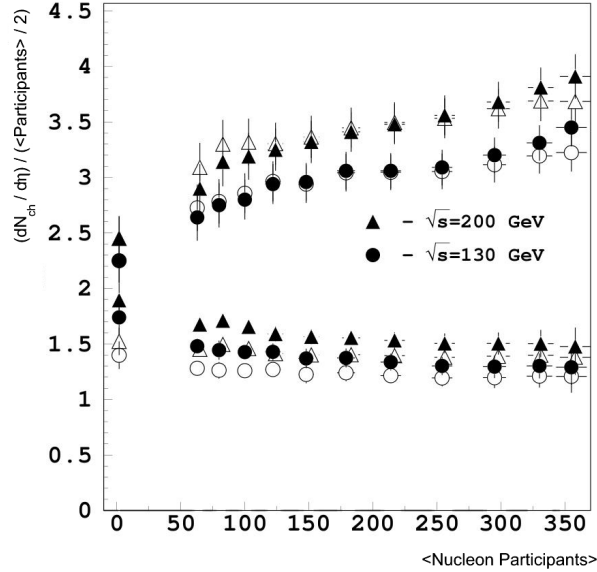
Figure 3: The ratio of produced charged particles per pseudorapidity unit at midrapidity $dN_{ch}/d\eta$ ($|\eta| < 1$) to the number of nucleon participant pairs $\langle N_{part} \rangle /2$ (at the top) and quark participant pairs $\langle Q_{part} \rangle /2$ (at the bottom) are plotted at a center-of-mass energy of $\sqrt{s_{NN}} = 130\,\text{GeV}$ and $\sqrt{s_{NN}} = 200\,\text{GeV}$ (RHIC-energy, Au+Au collisions) versus the number of nucleon participants N_{part}. The cross section (solid symbols) were chosen as $\sigma_{nn} = 41\,\text{mb}$ (nucleon-nucleon), $\sigma_{qq} = 4.56\,\text{mb}$ (quark-quark) at $\sqrt{s_{NN}} = 130\,\text{GeV}$ and $\sigma_{nn} = 42\,\text{mb}$, $\sigma_{qq} = 4.67\,\text{mb}$ at $\sqrt{s_{NN}} = 200\,\text{GeV}$. For the open symbols different cross sections are applied. We see that the number of quark participants is proportional to the multiplicity, whereas nucleon participants are not. Plot taken from [EV03]. The labels of the axes are modified.

Figure 3 emphasizes that the multiplicity does not scale with the nucleon participants but with the quark participants, because the ratio of produced particles at midrapidity over the quark participant pairs is approximately constant with respect to the nucleon participants.

This observation raises the question whether the scaling with the number of constituent quark participants also holds at LHC energies and for other reaction systems (e.g. p+Au (proton-gold), d+Au (deuteron-gold) and Pb+Pb(lead-lead)).

3 Theoretical Background

In this section some basic concepts and definitions of heavy-ion physics are introduced in order to describe heavy-ion collisions.

3.1 Nucleon and Quark Participants, Impact Parameter

In ultra-relativistic heavy-ion collisions, in which the nucleon mass is much smaller than the energy per nucleon in the center-of-mass system, the nucleons can be divided in a simple geometric picture into two groups: The spectator nucleons (N_{spec}) which do not interact with any other nucleon and the nucleon participants (N_{part}) which undergo at least one inelastic nucleon collision (N_{coll}) [Flo10]. The distance between the centers of two colliding nuclei is called impact parameter b, see Figure 4.
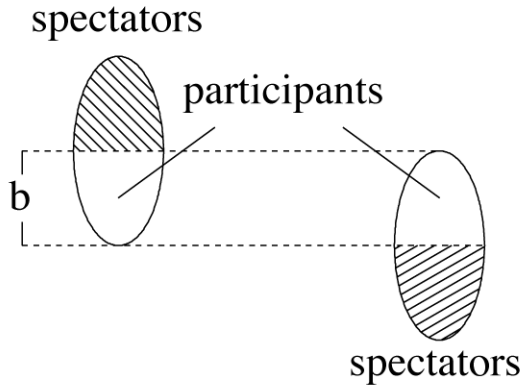
Figure 4: Nucleon participants and spectator nucleons at a given impact parameter b.

In the constituent participant model nucleons consists of 3 constituent quarks. We define quark participants (Q_{part}) as quark constituents which have suffered at least one inelastic quark collision (Q_{coll}).

3.2 Rapidity and Pseudorapidity

It is useful to introduce the rapidity as a measure of longitudinal velocity. The rapidity is additive with respect to Lorentz boosts. It is defined via:

$$y = \operatorname{arctanh} \beta_{\|} = \operatorname{arctanh} \left(\frac{p_{\|}}{E}\right) = \frac{1}{2} \ln \frac{(E + p_{\|})}{(E - p_{\|})} \tag{1}$$

where $E = \sqrt{m^2 + \vec{p}^2}$ is the total energy of the particle, $p_{\|}$ is the momentum in beam direction (longitudinal momentum) and $p_{\perp}$ is the transverse momentum

with $\vec{p}^2 = p_\perp^2 + p_\parallel^2$ and m is the particle's rest mass.

The energy and the momentum in beam direction (longitudinal momentum) can be calculated from the transverse mass $m_\perp = \sqrt{m^2 + p_\perp^2}$ and the rapidity as:

$$E = p^0 = m_\perp \cosh y \tag{2}$$

$$p_\parallel = m_\perp \sinh y \tag{3}$$

Multiplicity measurements are typically performed in limited windows of the pseudorapidity η (corresponding to a certain solid angle). For instance, multiplicity measurements at midrapidity correspond to $|\eta| < 1$. We introduce the η by the equation:

$$\eta = -\ln\left(\tan\frac{\theta}{2}\right) = \frac{1}{2}\ln\frac{(|\vec{p}| + p_\parallel)}{(|\vec{p}| - p_\parallel)} \tag{4}$$

where θ is the angle of the scattered particle with respect to the beam direction.

3.3 The Glauber Model

The Glauber model is applied to calculate the number of nucleon or quark participants. There are two different types of the Glauber model. In the optical Glauber model, the number of nucleon and quark participants can be analytically calculated from so-called thickness and nuclear overlap functions. This is in contrast to the Glauber-Monte-Carlo (GMC) approach, where the number of nucleon and quark participants is simulated by means of a Monte-Carlo algorithm. Within this thesis the GMC approach is chosen.

In the Glauber model nucleons are considered to act statically, which means that there is no motion of nucleons before or after a collision. Another assumption is that the nucleon-nucleon cross section (σ_{nn}) does not change no matter how many collisions the nucleon underwent before. Differences between protons and neutrons are not relevant and can be neglected in this simple model [RS11, MRSS07]. Hence, the measured charge density of a proton is used as an estimate for the neutron's density.

Details concerning the GMC simulation are described in Section 4.

3.4 Centrality

The number of nucleon and quark participants is calculated in simulations for different values of the impact parameter b. It is obvious that the impact parameter

characterizes the centrality of an A+A collision. However, the impact parameter is not directly measurable and represents only a theoretical quantity.

The number of nucleon participants obtained by simulations (see Section 4.1) is often used as a measure to describe the centrality of a collision. This can be done because the number of nucleon participants depends monotonically on the impact parameter (see Figure 9). It is assumed that the number of nucleon participants corresponds to the measured multiplicity.
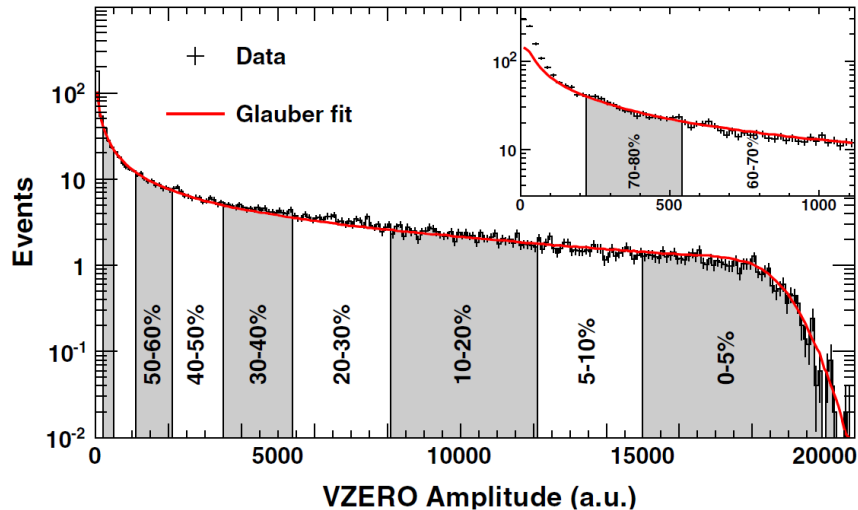
Figure 5: The number of Pb+Pb collisions at $\sqrt{s_{\mathrm{NN}}} = 2.76\,\mathrm{TeV}$ is plotted versus the VZERO Amplitude, which is proportional to the charged particle multiplicity. The inset shows the low amplitude part of the distribution. The red curve shows a Glauber model fit to the measurement. Plot taken from [Col11a].

Figure 5 illustrates how centrality classes can be defined in heavy-ion collisions. A mean number of nucleon participants can be assigned to each centrality class. With the monotonic relation between multiplicity, nucleon participants and impact parameter, it is possible to subdivide the multiplicity into percentiles [MRSS07].

3.5 The Diquark Model

In the diquark model nucleons consist of two constituents, a quark and a di-quark, see [Bia08, Bia12, APE+93]. The quark-quark (σ_{qq}), quark-diquark (σ_{qd}) and diquark-diquark (σ_{dd}) cross sections can assumed to be either equal (see Section 5.3) or different (see Section 5.4). In case that they are chosen differently the following condition has to be fulfilled:

$$\sigma_{\mathrm{qd}} = \pi \left(\frac{1}{2} \left(\sqrt{\frac{\sigma_{\mathrm{qq}}}{\pi}} + \sqrt{\frac{\sigma_{\mathrm{dd}}}{\pi}} \right) \right)^2 \tag{5}$$

8

3.6 Theoretical Basics of the Constituent Participant Model

Particle production processes can be phenomenologically described in a constituent participant model. The goal of this chapter is to sketch its theoretical justification [Bia12].

We consider a particle created in a high-energy collision of two ions in the reference frame in which the particle does not carry any longitudinal momentum: The irreducible time required for the formation of the particle is given by the uncertainty principle:

$$t_0 \geq \frac{1}{m_\perp} \tag{6}$$

In this frame $m_\perp = \sqrt{m^2 + p^2_\perp}$ is the energy of the particle.

In the frame in which the target nucleus is at rest the produced particle carries some longitudinal momentum such that the formation time is given by the equation:

$$t = \gamma\, t_0 \geq \frac{E}{m_\perp^2} = \frac{\cosh y_{\mathrm{lab}}}{m_\perp} \tag{7}$$

where E is the particle's energy and Equation (2) is used.

A formation length L is connected to the formation time within the particle is produced:

$$L = v\, t \geq \frac{\sinh y_{\mathrm{lab}}}{m_\perp} \tag{8}$$

where Equation (3) is used.

If the produced particle is fast enough, such that the formation length L is greater than the size of the colliding nuclei at a given impact parameter, the particle is not able to resolve any other collision. Hence, it is reasonable to assume that particle production is independent of the number of collisions the source underwent.

As a simple example we consider a p+p (proton-proton) collision at $\sqrt{s_{\mathrm{NN}}} = 200\,\mathrm{GeV}$. In this case the corresponding formation length is $L = 55\,\mathrm{fm}$. A typical diameter of a nucleus is about several fm (for gold about $14\,\mathrm{fm}$, for instance). Thus the size of the nucleus is much smaller than the formation length. Therefore it is reasonable to apply the constituent participant model to ultra-relativistic heavy-ion collisions.

4 Methods

The objective of this thesis is to study the particle production process in heavy-ion collisions with the constituent participant model. To this end the number of nucleon and quark participants in heavy ion-collisions has to be calculated.

In the following the concept of Glauber-Monte-Carlo simulation (GMC) is introduced which allows us to determine the number of nucleon and quark participants for different values of the impact parameter.

The number of produced particles in heavy-ion collisions was measured in experiments at the particle accelerators RHIC (Relativistic Heavy Ion Collider at Brookhaven National Laboratory) and LHC (Large Hadron Collider at CERN).

The measured multiplicities are combined with the number of nucleon and quark participants to study the scaling behavior of particle production.

4.1 Monte-Carlo Simulations

The number of nucleon and quark participants, as well as the impact parameter are quantities, which are not directly measurable. One way to obtain these quantities is to simulate heavy-ion collisions by means of Glauber-Monte-Carlo simulations. More precisely: At first the nucleons inside the nucleus are distributed. Therefore a coordinate system and spherical coordinates (r, φ, ϑ) are defined. Then the distances r_n of the nucleons to the origin are randomly drawn from a nuclear charge density distribution (see Section 4.2). Secondly, the quarks inside a nucleon are distributed. Therefore the distances r_q of the quarks to the center of the nucleon are randomly drawn from a nucleon charge density distribution (see Section 4.3). Afterwards for nucleons and quarks, respectively, the angles φ_n, ϑ_n, φ_q, and ϑ_q, related to the coordinates of nucleons and quarks, are randomly drawn to fix the position in space for each particle.

After that a second nucleus is simulated in the same way, however, with a certain transverse distance to the first nucleus. This distance is the impact parameter b, randomly drawn from the distribution:

$$\frac{\mathrm{d}\sigma}{\mathrm{d}b} = 2\pi b \tag{9}$$

Finally, for each nucleon and quark, respectively, it is tested whether a collision happens, or not (see Section 4.4). The number of participants is counted.

This entire procedure is repeated between 4000 and 40000 times. The number of quark and nucleon participants are grouped into percentiles. Then all participants within a percentile are averaged.

4.2 Nucleon Distribution

In order to distribute the nucleons inside the nucleus a Woods-Saxon nuclear charge density function is chosen and multiplied with the surface of a sphere with radius r [MRSS07]. The product yields the number of nucleons per radius interval $\mathrm{d}r$:

$$\frac{\mathrm{d}N}{\mathrm{d}r} = \rho(r) \cdot \frac{\mathrm{d}V}{\mathrm{d}r} = \frac{\rho_0(1 + wr^2/R^2)}{1 + \exp((r - R)/a)} \cdot 4\pi r^2 \tag{10}$$

where R is the radius of the nucleus, a is the "skin thickness", $w > 0$ describes a profile for which the maximum density is reached at radius $r > 0$ and ρ_o is the nucleon density in the middle of the nucleus. Figure 6 illustrates the Woods-Saxon distribution.
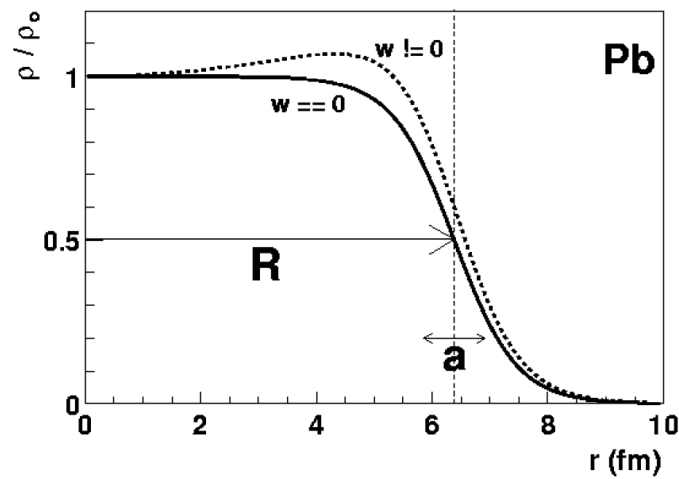
Figure 6: Woods-Saxon nuclear charge density ρ/ρ_0 as a function of the radius r. The impact of different parameter values is illustrated. R represents the radius of the nucleus, a the "skin thickness", $w > 0$ describes a profile for which the maximum density is reached at radius $r > 0$ and ρ_o the nucleon density in the middle of the nucleus. Plot taken from [RS11].

For gold (Au) and lead (Pb) the following values are chosen [DVDJDV87]:

Nucleus	Mass number A	Radius R (fm)	a (fm)	w
Au	197	6.38	0.535	0
Pb	208	6.62	0.546	0

11

4.3 Quark Distribution

In the constituent participant model each nucleon consists of 3 constituent quarks. In order to distribute the quarks within a nucleon an exponential particle distribution function is chosen and multiplied with the surface of a sphere with radius r [PRSZ99]. The product yields the number of quarks per radius interval $\mathrm{d}r$:

$$\frac{\mathrm{d}N}{\mathrm{d}r} = \rho(r) \cdot \frac{\mathrm{d}V}{\mathrm{d}r} = \rho_0 \cdot \exp(-ar) \cdot 4\pi r^2 \tag{11}$$

A value of $a = 4.27\,\mathrm{fm}^{-1}$ is used in the calculation.

4.4 Collisions of Nuclei

Figure 7 shows the nucleon distributions for two colliding Pb nuclei for a randomly set impact parameter of 6 fm.
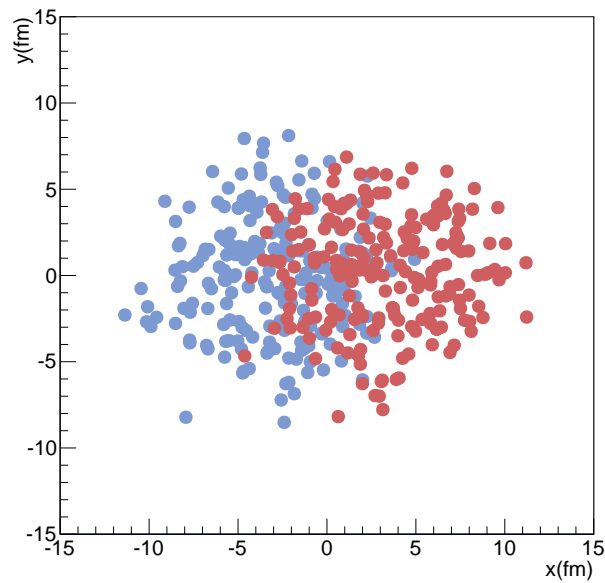
Figure 7: Nucleon distributions for two colliding Pb nuclei for a randomly set impact parameter of 6 fm.

The next step, after the creation of two nuclei at transverse distance b, is to formulate a collision condition. The quarks and nucleons are regarded as black disks. A collision takes place whenever the distance d of two constituents fulfills:

$$d \leq \sqrt{\frac{\sigma}{\pi}} \tag{12}$$

where σ is the cross section of a nucleon or quark. Figure 8 demonstrates this situation.
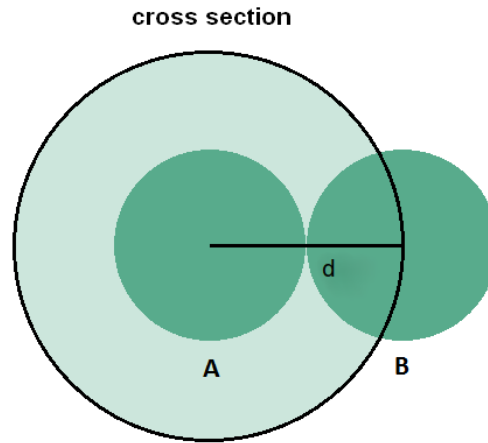
cross section

Figure 8: Nucleon (quark) A with radius r collides with nucleon (quark) B with the same radius. The distance $d_{\mathrm{max}} = 2r$ is the maximum distance for which a collision takes place. The cross section of the collision $\sigma = \pi d_{\mathrm{max}}^2$ corresponds to a disk with radius d_{max}.

The values for the nucleon-nucleon cross sections (σ_{nn}) were measured in different p+p scattering experiments, see [A$^+$86, Col11a]. Either the inelastic cross section or the non-diffractive cross section is used. For the inelastic cross section diffractive processes, in which a pomoron is exchanged as well as non-diffractive processes are considered. In Section 5 both cross section are used. The relation between these cross sections is given by:

$$\sigma_{\mathrm{inel}} = \sigma_{\mathrm{nd}} + \sigma_{\mathrm{sd}} + \sigma_{\mathrm{dd}} + \sigma_{\mathrm{cd}} \tag{13}$$

where σ_{inel} is the inelastic cross section, σ_{nd} is the non-diffractive cross section, σ_{sd} is the single diffractive cross section, σ_{dd} is the double diffractive cross section and σ_{cd} is the central diffractive cross section.

For instance, in p+p̄ (proton-antiproton) collisions at $\sqrt{s_{\mathrm{NN}}} = 200\,\mathrm{GeV}$ the following values were measured [RS11, A$^+$86]:

$\sigma_{\mathrm{inel}}\,(\mathrm{mb})$	$\sigma_{\mathrm{nd}}\,(\mathrm{mb})$	$\sigma_{\mathrm{sd}}\,(\mathrm{mb})$	$\sigma_{\mathrm{dd}}\,(\mathrm{mb})$	$\sigma_{\mathrm{cd}}\,(\mathrm{mb})$
41.8 ± 0.6	≈ 33.5	$4.8 \pm 0.5 \pm 0.8$	3.5 ± 2.2	< 1

The values for the quark-quark cross section (σ_{qq}), which cannot be measured for A+A collisions, can be either obtained via tuning the quark cross section in such a way that the nucleon-nucleon cross section is reproduced (see Figure 10) or the nucleon-nucleon cross section is divided by 9 to obtain the quark-quark cross section. This idea has its origin in the additive quark model in which the nucleon-nucleon, nucleon-quark and quark-quark cross sections are given by: $\sigma_{\mathrm{nn}} = 3 \cdot \sigma_{\mathrm{nq}}$ and $\sigma_{\mathrm{qn}} = 3 \cdot \sigma_{\mathrm{qq}}$ [BCL82].
Additionally it is also possible to set the quark-quark cross section as a free parameter. This is of particular importance for the diquark model (see Section 3.5).

4.5 Input Parameters

The number of produced particles in heavy-ions collisions in Au+Au collisions was measured by the experiments PHENIX [AAA$^+$05] and PHOBOS [Col11b] at the RHIC. In Section 5 also p+p and d+Au (deuteron-gold) collisions measured at the RHIC are analyzed [Col11b]. Additionally Pb+Pb (lead-lead) collisions are studied which were recently measured by the ALICE experiment at the LHC [Col11a]. In these experiments the multiplicity at midrapidity ($|\eta| < 0.5$ (LHC) or $|\eta| < 1$ (RHIC)) is examined as well as the total charged particle multiplicity ($|\eta| < 5.4$ (RHIC)).

5 Results

The objective of this thesis is to test the constituent participant model. The model is tested with data from different experiments at different energies, see Section 4.5. We start with a discussion of basic results of the constituent participant model.

5.1 Basic Results of the Constituent Participant Model

5.1.1 Nucleon and Quark Participants

In this section nucleon and quark participants N_{part}, Q_{part} as well as nucleon and quark collisions N_{coll}, Q_{coll} are discussed. The relations between these quantities and their dependence on the impact parameter are analyzed.
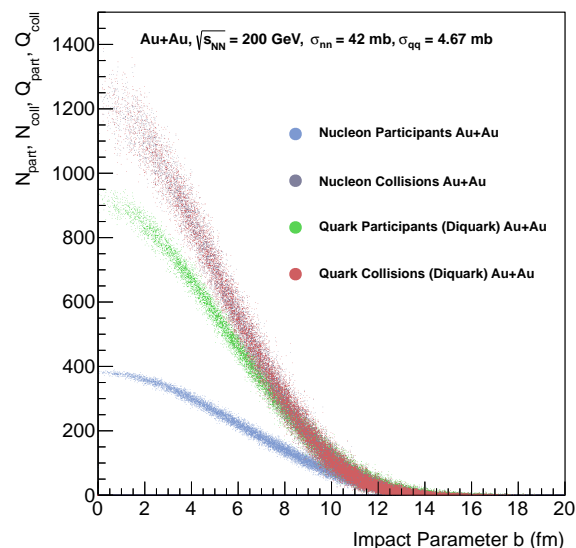
Figure 9: The simulated number of nucleon and quark participants N_{part}, Q_{part} as well as the number of nucleon and quark collisions N_{coll}, Q_{coll} for Au+Au collisions at $\sqrt{s_{\text{NN}}} = 200\,\text{GeV}$ are plotted as a function of the impact parameter for $\sigma_{\text{nn}} = 42\,\text{mb}$ and $\sigma_{\text{qq}} = 4.67\,\text{mb}$. In this calculation nucleons have 3 constituent quarks.

From Figure 9 we find as expected, in central Au+Au collision about 400 nucleon participants and about 900 quark participants. Almost all nucleons ($2 \cdot 197 = 394$) but not all quarks ($2 \cdot 3 \cdot 197 = 1182$) participate in this collision of two gold nuclei. This is because the quark-quark cross section ($\sigma_{\text{qq}} = 4.67\,\text{mb}$) is much smaller than the nucleon-nucleon cross section ($\sigma_{\text{nn}} = 42\,\text{mb}$).
In addition we find that the number of nucleon and quark collisions is quite similar.

This is due to the fact that even though there are much more quark participants than nucleon participants, the quark-quark cross section is much smaller than the nucleon-nucleon cross section. Hence, quarks often do not interact with their neighbor quarks.

Furthermore, we see that for an increasing impact parameter the number of nucleon and quark participants as well as the number of nucleon and quark collisions decreases.

5.1.2 Reproduction of σ_{nn} via Tuning σ_{qq}

In this thesis 3 approaches are chosen to determine the quark-quark cross section. One way is to tune the quark-quark cross section until the total cross section of a nucleon composed of 3 quarks reproduces the experimental measured nucleon-nucleon (p+p) cross section at the corresponding energy.
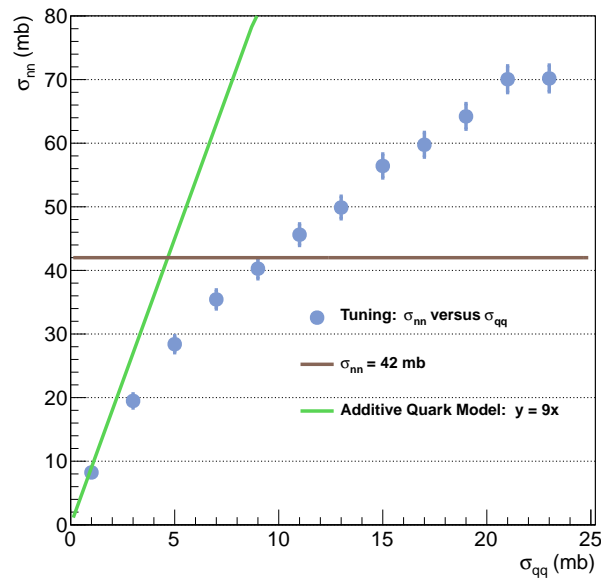
Figure 10: The nucleon-nucleon cross section (σ_{nn}) is plotted versus the quark-quark cross section (σ_{qq}). In green the relation $y = (3 \cdot 3)\, x$, which describes the quark-quark cross section in the additive quark model, see Section 4.4. In gray the inelastic nucleon-nucleon cross section of $\sigma_{nn} = 42\,\text{mb}$ at $\sqrt{s_{NN}} = 200\,\text{GeV}$.

There is a difference between quark-quark cross sections obtained from tuning and quark-quark cross sections obtained from the additive quark model, see Figure 10. For instance we find for $\sigma_{nn} = 42\,\text{mb}$ from tuning $\sigma_{qq} = 9\,\text{mb}$ and from the additive quark model $\sigma_{qq} = 4.67\,\text{mb}$.

5.2 The Constituent Participant Model

In the following the constituent participant model with 3 constituents is tested. We test whether the multiplicity in heavy-ion collisions is proportional to the number of participating constituent quarks or not.

5.2.1 Particle Production at Midrapidity in Au+Au Collisions

At first it shall be demonstrated that the model developed within this thesis reproduces the results by Eremin and Voloshin [EV03].
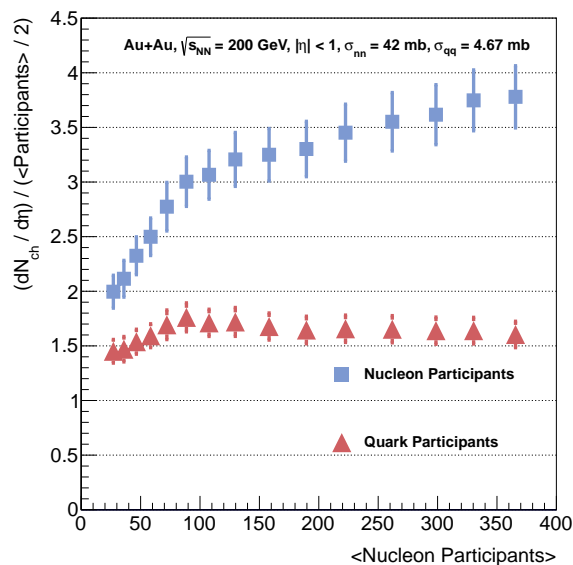
Figure 11: The ratio of produced charged particles per pseudorapidity unit at midrapidity $dN_{ch}/d\eta$ ($|\eta| < 1$) to the number of nucleon participant pairs $\langle N_{part}\rangle/2$ (at the top) and quark participant pairs $\langle Q_{part}\rangle/2$ (at the bottom) are plotted at a center-of-mass energy of $\sqrt{s_{NN}} = 200\,\text{GeV}$ (RHIC-energy, Au+Au collisions) versus the number of nucleon participants N_{part} for $\sigma_{nn} = 42\,\text{mb}$ and $\sigma_{qq} = 4.67\,\text{mb}$. We see that the applied simulation yields the same result in comparison to Figure 3.

In Figure 11 we see the same shape and values of the plotted data in agreement with errors as in Figure 3.
In addition we see that in Figure 3 peripheral data points are missing (with about 10 to 70 nucleon participants). This is due to the fact that these points were not available at the time of this publication.
We find in Figure 11 that for peripheral collisions the multiplicity does not scale with the number of quark participants.

In Figure 12 the same multiplicity data are shown for a different quark-quark cross section. This is done to examine the impact of σ_{qq} on the ratio of multiplicity to quark participant pairs. The quark-quark cross section of $\sigma_{qq} = 9\,\mathrm{mb}$ which we found in the tuning is used (see Section 5.1.2).
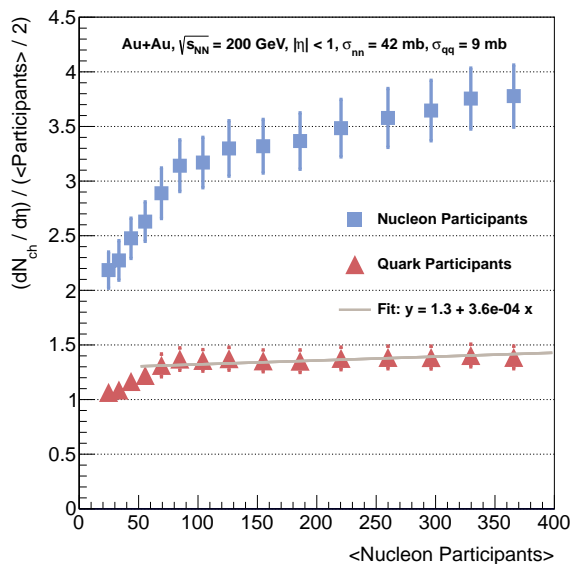
Figure 12: The ratio of produced charged particles per pseudorapidity unit at midrapidity $\mathrm{d}N_{\mathrm{ch}}/\mathrm{d}\eta$ ($|\eta| < 1$) to the number of nucleon participant pairs $\langle N_{\mathrm{part}} \rangle /2$ (at the top) and quark participant pairs $\langle Q_{\mathrm{part}} \rangle /2$ (at the bottom) are plotted at a center-of-mass energy of $\sqrt{s_{\mathrm{NN}}} = 200\,\mathrm{GeV}$ (RHIC-energy, Au+Au collisions) versus the number of nucleon participants N_{part} for $\sigma_{\mathrm{nn}} = 42\,\mathrm{mb}$ and $\sigma_{\mathrm{qq}} = 9\,\mathrm{mb}$. The data points for the quark participants are fitted by a straight line in the range of 50 to 400 nucleon participants.

In Figure 12 we find that the ratio of multiplicity to quark participant pairs is on average smaller than in Figure 11. This is due to the larger value of the quark-quark cross section. Hence, there are more quark participants. In addition we see a slightly increasing ratio of multiplicity over quark participant pairs for an increasing number of nucleon participants.

In the next step the ratio of multiplicity to quark participant pairs is quantitatively analyzed as a function of σ_{qq}. Therefore further plots are made for different values of σ_{qq}. In these plots the data for the quark participants are fitted by a straight line in the range from 50 to 400 nucleon participants as already shown in Figure 12. The result is shown in Figure 13.
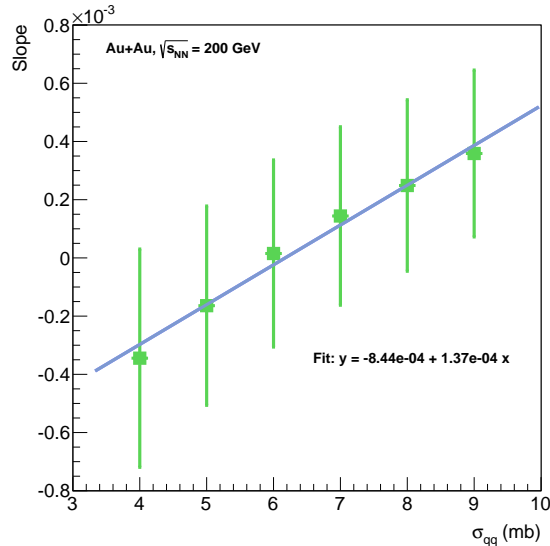
Figure 13: The slope of the fitted straight lines in the range from 50 to 400 nucleon participants of the plots in which the ratio of multiplicity to quark participant pairs versus nucleon participants for different values of σ_{qq} is plotted versus σ_{qq}. For $\sigma_{qq} = 6.17$ mb the slope is totally flat.

Figure 13 shows that for $\sigma_{qq} = 6.17$ mb the slope of the fitted straight line in the plot in which the ratio of multiplicity to quark participant pairs versus nucleon participants is plotted versus σ_{qq} becomes totally flat in the fitting range. Hence, the multiplicity is proportional to the number of quark participants. For $\sigma_{qq} = 6.17$ mb the constituent participant model describes particle production. We also find that the scaling for $\sigma_{qq} = 4.67$ mb, obtained from the additive quark model and $\sigma_{qq} = 9$ mb obtained from tuning, only works approximately. Therefore we abandon the approach of reproducing the p+p cross section to obtain σ_{qq} as well as the approach to calculate σ_{qq} from the additive quark model. In the following the quark-quark cross section is regarded as a free parameter.

In the next step a different value for the nucleon-nucleon cross section is applied. Instead of the inelastic value of $\sigma_{nn} = 42$ mb, the non-diffractive cross section of $\sigma_{nn} = 33.5$ mb is used (see Section 4.4). The same procedure done for the inelastic nucleon-nucleon cross section is now repeated for the non-diffractive one. We find

that the multiplicity is proportional to the number of quark participants when a quark-quark cross section of $\sigma_{qq} = 4.50\,\text{mb}$ is used.

For the considered Au+Au collisions at $\sqrt{s_{NN}} = 200\,\text{GeV}$ at midrapidity it is always possible to find a value for σ_{qq} for which the slope becomes totally flat.

5.2.2 Particle Production at Midrapidity in Pb+Pb Collisions

In the previous section, it is shown that for Au+Au collisions at midrapidity and $\sqrt{s_{NN}} = 200\,\text{GeV}$ the constituent participant model works for not too peripheral collisions. This is in total agreement with the result published by Eremin and Voloshin [EV03]. In the next step the constituent participant model is tested in Pb+Pb collisions at midrapidity and $\sqrt{s_{NN}} = 2.76\,\text{TeV}$. In Figure 14 the ratio of multiplicity to the number of quark and nucleon participants is plotted versus the number of nucleon participants for a value of $\sigma_{qq} = 7.11\,\text{mb}$.
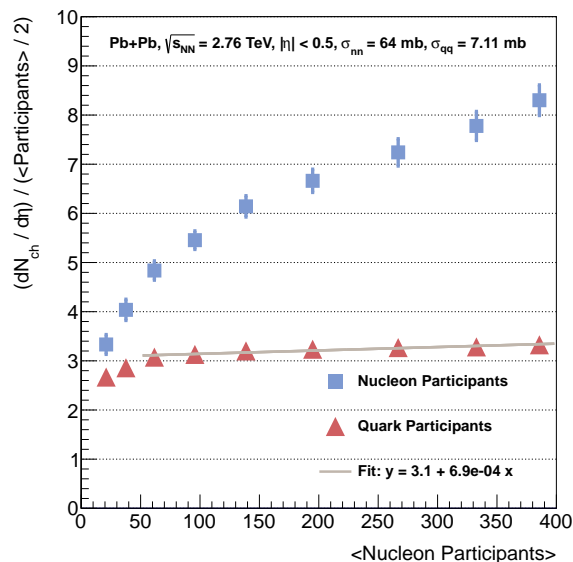
Figure 14: The ratio of produced charged particles per pseudorapidity unit at midrapidity $dN_{ch}/d\eta$ ($|\eta| < 0.5$) to the number of nucleon participant pairs $\langle N_{part}\rangle /2$ (at the top) and quark participant pairs $\langle Q_{part}\rangle /2$ (at the bottom) are plotted at a center-of-mass energy of $\sqrt{s_{NN}} = 2.76\,\text{TeV}$ (LHC-energy, Pb+Pb collisions) versus the number of nucleon participants N_{part} for $\sigma_{nn} = 64\,\text{mb}$ and $\sigma_{qq} = 7.11\,\text{mb}$.

In Figure 14 we see that the ratio of multiplicity to quark participant pairs slightly increases with an increasing number of nucleon participants.

In order to analyze the scaling behavior quantitatively as a function of σ_{qq} further

plots were made for different values of σ_{qq}. In these plots the data for quark partic-ipants are fitted by a straight line in the range from 50 to 400 nucleon participants. The result is shown in Figure 15.
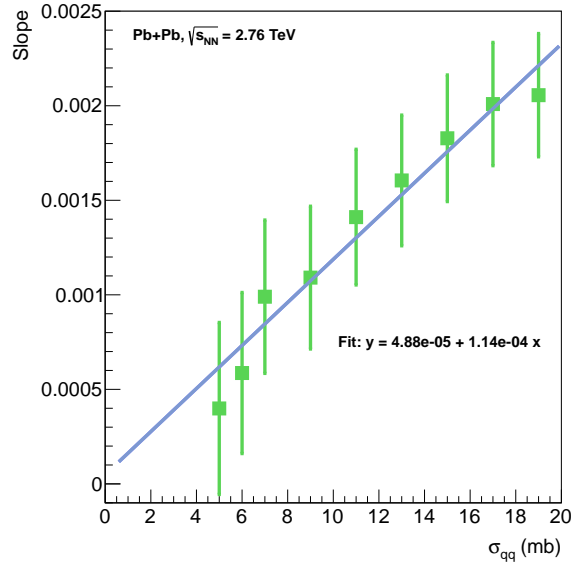
Figure 15: The slope of the fitted straight lines in the range from 50 to 400 nucleon participants of the plots in which the ratio of multiplicity to quark participant pairs versus nucleon participants for different values of σ_{qq} is plotted versus σ_{qq}. We see that there is no value for σ_{qq} for which the slope becomes totally flat.

Figure 15 shows the slope of the straight line in the multiplicity plots versus the used value for the quark-quark cross section σ_{qq}. No value for the quark-quark cross section can be found for which the slope becomes totally flat.
The constituent participant model does not describe the multiplicity in Pb+Pb collisions at $\sqrt{s_{\mathrm{NN}}} = 2.76 \, \mathrm{TeV}$. This is in contrast to the results shown for Au+Au collisions at $\sqrt{s_{\mathrm{NN}}} = 200 \, \mathrm{GeV}$ where the constituent participant model describes the particle production for not too peripheral collisions.

5.2.3 Total Charged Multiplicity in d+Au Collisions

In the following the total charged multiplicity N_{ch} in d+Au collisions at $\sqrt{s_{\mathrm{NN}}} = 200 \, \mathrm{GeV}$ measured in $|\eta| < 5.4$ is analyzed with the constituent participant model instead of the multiplicity measured at midrapidity ($|\eta| < 1$). The total multi-plicity is measured within a much larger solid angle range.

21

Hence, the total multiplicity is less biased by centrality dependent effects affecting the shape of the $dN_{ch}/d\eta$ distribution.
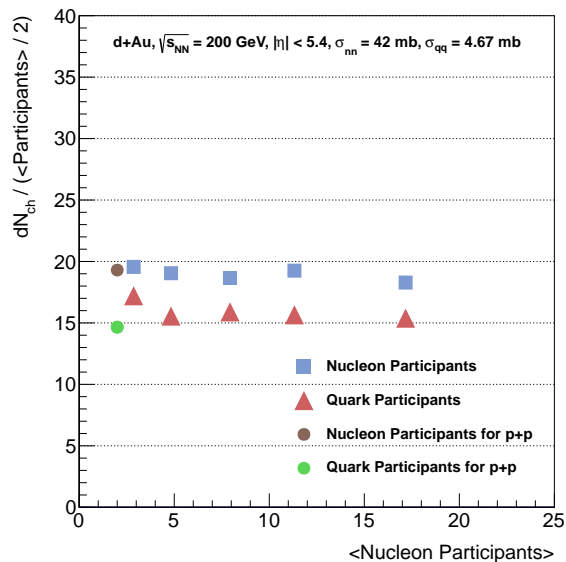
Figure 16: The ratio of total charged multiplicity dN_{ch} ($|\eta| < 5.4$) to the number of nucleon participant pairs $\langle N_{part} \rangle /2$ (at the top) and quark participant pairs $\langle Q_{part} \rangle /2$ (at the bottom) are plotted at a center-of-mass energy of $\sqrt{s_{NN}} = 200\,\text{GeV}$ (RHIC-energy, p+p, d+Au collisions) versus the nucleon participants N_{part} for $\sigma_{nn} = 42\,\text{mb}$ and $\sigma_{qq} = 4.67\,\text{mb}$.

As already mentioned in Section 2.1 the starting point for the constituent participant model is the observation that the multiplicity in p+A collisions is proportional to the number of nucleon participants. One would expect to see this proportionality in d+Au collisions which should behave quite similar as p+A collisions.

In Figure 16 a value of $\sigma_{qq} = 4.67\,\text{mb}$ is chosen for which the constituent participant model describes the data best. In addition also the p+p point is plotted, where the measured total charged multiplicity in p+p collisions has been divided by the mean number of quarks participating (same value for σ_{qq}).
We find that both the nucleon and the quark participants scale approximately with the number of produced particles. The expectation for the nucleon participants can be confirmed.
Furthermore the p+p point is in accord with the ratio, multiplicity to quark participant pairs for the d+Au collisions. We find a consistent description of p+p and d+Au collisions in the constituent participant model. The next step is to test this value for σ_{qq} in Au+Au collisions.

5.2.4 Total Charged Multiplicity in Au+Au Collisions

In this section the total charged multiplicity in Au+Au collisions is studied.
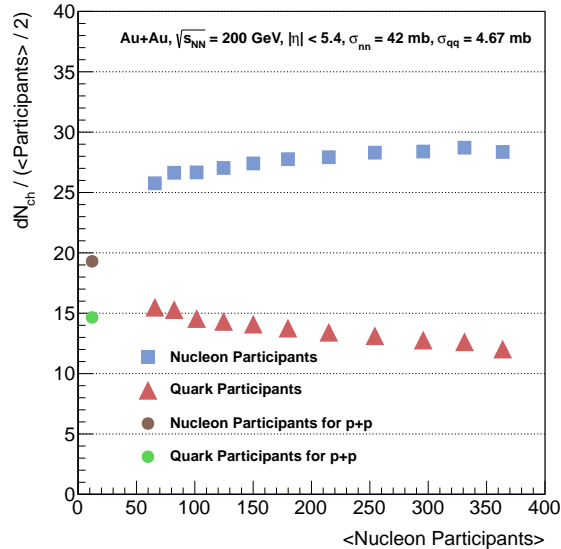
Figure 17: The ratio of total charged multiplicity dN_{ch} ($|\eta| < 5.4$) to the number of nucleon participant pairs $\langle N_{part} \rangle /2$ (at the top) and quark participant pairs $\langle Q_{part} \rangle /2$ (at the bottom) are plotted at a center-of-mass energy of $\sqrt{s_{NN}} = 200\,\text{GeV}$ (RHIC-energy, p+p, Au+Au collisions) versus the nucleon participants N_{part} for $\sigma_{nn} = 42\,\text{mb}$ and $\sigma_{qq} = 4.67\,\text{mb}$.

In Figure 17 we find a consistency between the p+p point and the ratio of multiplicity to quark participant pairs for peripheral Au+Au collisions. The same number of particles per quark participant pair is created in peripheral Au+Au collision and in p+p collisions. This is in agreement with the picture that in peripheral Au+Au collision actually single nucleons collide.
Finally it is obvious that the multiplicity does not scale with the number of quark participants for a quark-quark cross section of $\sigma_{qq} = 4.67\,\text{mb}$. Remarkable, because this is actually the cross section for which the scaling in Au+Au collision at midrapidity works (see Section 5.2.1).

In order to check whether a cross section exists for which the ratio of multiplicity to quark participants is approximately constant from peripheral to central collisions the value of σ_{qq} is varied. For $\sigma_{qq} = 30\,\text{mb}$ this is achieved. However, the applied quark-quark cross section of $\sigma_{qq} = 30\,\text{mb}$ is unrealistic, because the quark-quark cross section is almost as large as the nucleon-nucleon cross section $\sigma_{nn} = 42\,\text{mb}$. We emphasize that the constituent participant model is not consistent in the description of particle production for p+p, d+Au and Au+Au collisions.

5.2.5 Comparison of p+p, d+Au and Au+Au Collisions

In this section the results for p+p, d+Au and Au+Au collisions are displayed together in one single plot. Because the multiplicity scaling in d+Au collisions works best for $\sigma_{qq} = 4.67\,\text{mb}$ this value is used in Figure 18.
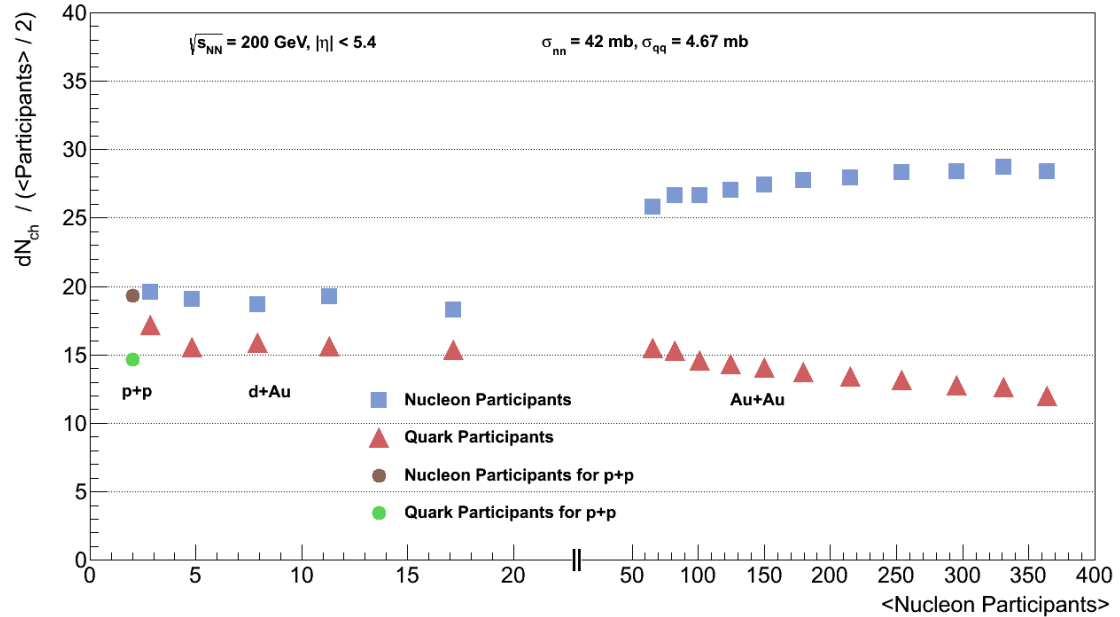
Figure 18: The ratio of total charged multiplicity dN_{ch} ($|\eta| < 5.4$) to the number of nucleon participant pairs $\langle N_{\text{part}} \rangle /2$ (at the top) and quark participant pairs $\langle Q_{\text{part}} \rangle /2$ (at the bottom) are plotted at a center-of-mass energy of $\sqrt{s_{\text{NN}}} = 200\,\text{GeV}$ for p+p, d+Au and Au+Au collisions versus N_{part}. The used cross sections are: $\sigma_{\text{nn}} = 42\,\text{mb}$, $\sigma_{\text{qq}} = 4.67\,\text{mb}$.

Figure 18 shows that for a quark-quark cross section of $\sigma_{\text{qq}} = 4.67\,\text{mb}$ the total charged multiplicity does scale in d+Au collisions, but does not scale in Au+Au collisions with the number of quark participants. There is only a consistency between p+p, d+Au and the peripheral Au+Au collisions.

Again, this plot shows that the total charged multiplicity in heavy-ion collisions does not scale consistently with three quark participants. The model of constituent participants proposed by Eremin and Voloshin does not consistently work.

5.3 The Diquark Model ($\sigma_{\mathbf{qq}} = \sigma_{\mathbf{qd}} = \sigma_{\mathbf{dd}}$)

In the following the so-called diquark participant model in which nucleons are composed of a quark and a diquark is studied. We test whether the diquark participant model describes particle production in heavy-ion collisions or not. At first we set $\sigma_{\mathrm{qq}} = \sigma_{\mathrm{qd}} = \sigma_{\mathrm{dd}}$, which means cross sections for quark-quark, quark-diquark and diquark-diquark interactions are identical.

5.3.1 Total Charged Multiplicity in d+Au Collisions

At first d+Au collisions at $\sqrt{s_{\mathrm{NN}}} = 200\,\mathrm{GeV}$ are examined. In order to get multiplicity scaling with respect to the number of quark participants, the quark-quark cross section is varied. For $\sigma_{\mathrm{qq}} = \sigma_{\mathrm{qd}} = \sigma_{\mathrm{dd}} = 12\,\mathrm{mb}$ the best result is found, see Figure 19.
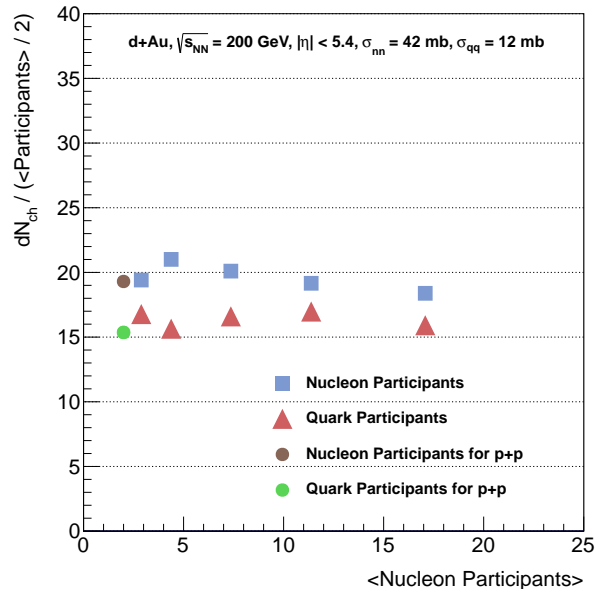
Figure 19: The ratio of total charged multiplicity dN_{ch} ($|\eta| < 5.4$) to the number of nucleon participant pairs $\langle N_{\mathrm{part}} \rangle /2$ (on the top) and quark participant pairs $\langle Q_{\mathrm{part}} \rangle /2$ (on the bottom) are plotted at $\sqrt{s_{\mathrm{NN}}} = 200\,\mathrm{GeV}$ for p+p and d+Au collisions versus the nucleon participants N_{part}. Used cross sections: $\sigma_{\mathrm{nn}} = 42\,\mathrm{mb}$, $\sigma_{\mathrm{qq}} = \sigma_{\mathrm{qd}} = \sigma_{\mathrm{dd}} = 12\,\mathrm{mb}$.

In Figure 19 we find that the total charged multiplicity does scale approximately with the number of quark participants in d+Au collisions. The p+p point is also consistent with the approximately constant ratio of multiplicity to quark participant pairs.

5.3.2 Total Charged Multiplicity in Au+Au Collisions

In Figure 20 the ratio of multiplicity to quark participant pairs is plotted against the number of nucleon participants for $\sigma_{qq} = \sigma_{qd} = \sigma_{dd} = 4.67\,\text{mb}$.
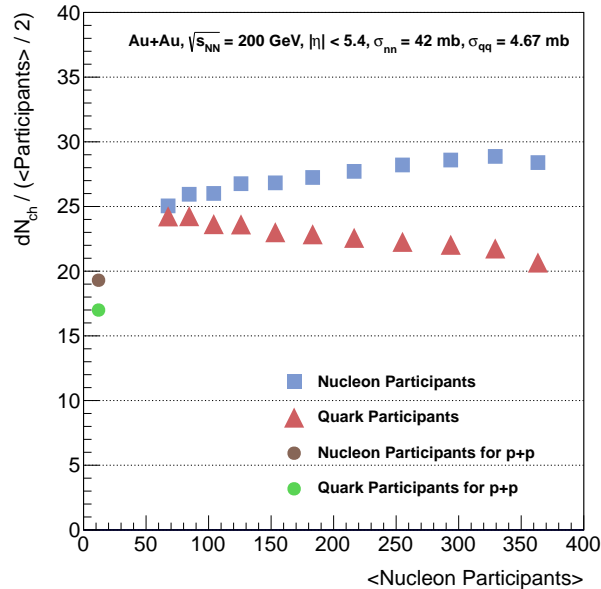
Figure 20: The ratio of total charged multiplicity dN_{ch} ($|\eta| < 5.4$) to the number of nucleon participant pairs $\langle N_{part} \rangle /2$ (at the top) and quark participant pairs $\langle Q_{part} \rangle /2$ (at the bottom) are plotted at a center-of-mass energy of $\sqrt{s_{NN}} = 200\,\text{GeV}$ (RHIC-energy, p+p and Au+Au collisions) versus the nucleon participants N_{part} for $\sigma_{nn} = 42\,\text{mb}$ and $\sigma_{qq} = \sigma_{qd} = \sigma_{dd} = 4.67\,\text{mb}$.

From Figure 20 we find that the multiplicity does not scale with the number of quark participants. However, one sees a similarity between Figure 17 and Figure 20. The slope of the decreasing ratio of multiplicity to quark participant pairs is quite similar. The difference is in Figure 17 nucleons have 3 constituents and in Figure 20 ony 2. When only 2 quarks are distributed we find less quark participants. However, the relative increase of quark participants for an increasing centrality is quite similar in the diquark and in the constituent participant model with 3 constituents.

In the next step the quark-quark cross section is varied until the ratio of multiplicity to quark participant pairs is constant from peripheral to central collisions.
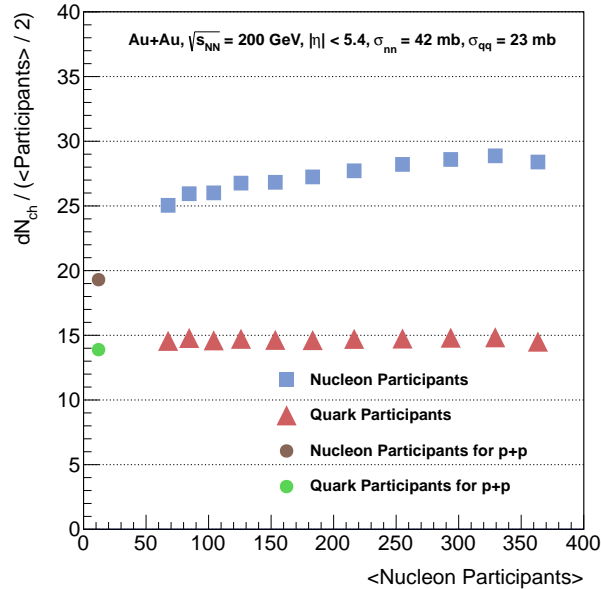
Figure 21: The ratio of total charged multiplicity dN_{ch} ($|\eta| < 5.4$) to the number of nucleon participant pairs $\langle N_{part} \rangle /2$ (at the top) and quark participant pairs $\langle Q_{part} \rangle /2$ (at the bottom) are plotted at a center-of-mass energy of $\sqrt{s_{NN}} = 200\,\text{GeV}$ (RHIC-energy, p+p and Au+Au collisions) versus the nucleon participants N_{part} for $\sigma_{nn} = 42\,\text{mb}$ and $\sigma_{qq} = \sigma_{qd} = \sigma_{dd} = 23\,\text{mb}$.

In Figure 21 a quark-quark cross section of $\sigma_{qq} = \sigma_{qd} = \sigma_{dd} = 23\,\text{mb}$ is used. The diquark model describes the total charged multiplicity in d+Au collisions. The p+p point is also consistent with the d+Au data.
However, we find from Figure 19 that in d+Au collisions the diquark participant model describes the data best for $\sigma_{qq} = \sigma_{qd} = \sigma_{dd} = 12\,\text{mb}$. Therefore we plot the data from p+p, d+Au and Au+Au collisions in one figure together.

5.3.3 Comparison of p+p, d+Au and Au+Au Collisions

The results for p+p, d+Au and Au+Au collisions with $\sigma_{\mathrm{qq}} = \sigma_{\mathrm{qd}} = \sigma_{\mathrm{dd}} = 12\,\mathrm{mb}$ are displayed together in Figure 22.
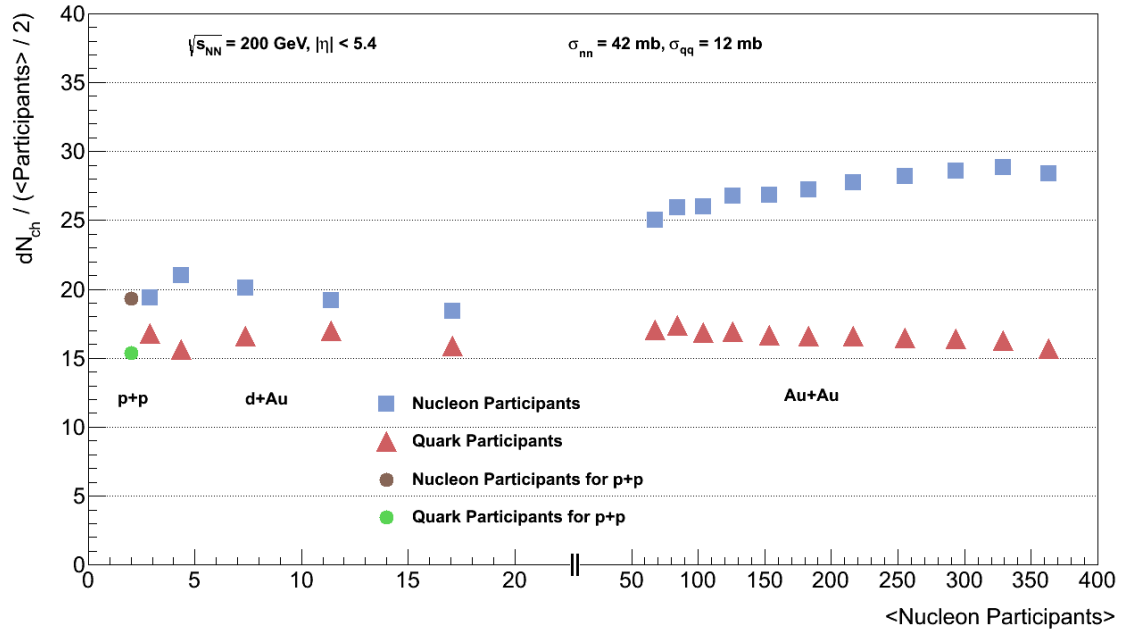
Figure 22: The ratio of total charged multiplicity $\mathrm{d}N_{\mathrm{ch}}$ ($|\eta| < 5.4$) to the number of nucleon participant pairs $\langle N_{\mathrm{part}} \rangle /2$ (at the top) and quark participant pairs $\langle Q_{\mathrm{part}} \rangle /2$ (at the bottom) are plotted at a center-of-mass energy of $\sqrt{s_{\mathrm{NN}}} = 200\,\mathrm{GeV}$ for p+p, d+Au and Au+Au collisions versus the nucleon participants N_{part}. The used cross sections are: $\sigma_{\mathrm{nn}} = 42\,\mathrm{mb}$, $\sigma_{\mathrm{qq}} = \sigma_{\mathrm{qd}} = \sigma_{\mathrm{dd}} = 12\,\mathrm{mb}$.

Figure 22 shows that the multiplicity scales approximately with the number of quark participants. Especially for peripheral Au+Au collisions the ratio of multiplicity to quark participant pairs is a little too large. However, we see a consistency in the plotted data from p+p,d+Au to central Au+Au collisions.

We find that the diquark constituent model approximately describes the total multiplicity in heavy-ion collisions whereas the constituent participant model with 3 quarks does not, see Figure 18 and Figure 22.

5.4 The Diquark Model ($\sigma_{\mathsf{qq}} \neq \sigma_{\mathsf{qd}}$ and $\sigma_{\mathsf{qq}} \neq \sigma_{\mathsf{dd}}$)

In the following the used cross sections for the quarks and diquarks are not equal anymore: $\sigma_{\mathrm{qq}} \neq \sigma_{\mathrm{qd}}$ and $\sigma_{\mathrm{qq}} \neq \sigma_{\mathrm{dd}}$.

5.4.1 Comparison of p+p, d+Au and Au+Au Collisions

In order to test the diquark model with different values for the quark-quark, quark-diquark and diquark-diquark cross sections we firstly vary these cross sections for the simulated d+Au collisions. This tuning is done until the ratio of total charged multiplicity to quark participant pairs is approximately constant as a function of the centrality (nucleon participants). The following values have turned out to work best: $\sigma_{\mathrm{qq}} = 8\,\mathrm{mb}$, $\sigma_{\mathrm{qd}} = 12.5\,\mathrm{mb}$, $\sigma_{\mathrm{dd}} = 18\,\mathrm{mb}$.

After simulating d+Au collisions for the same cross sections Au+Au collisions are simulated. The results for d+Au, Au+Au as well as the p+p point are plotted in one single plot, see Figure 23
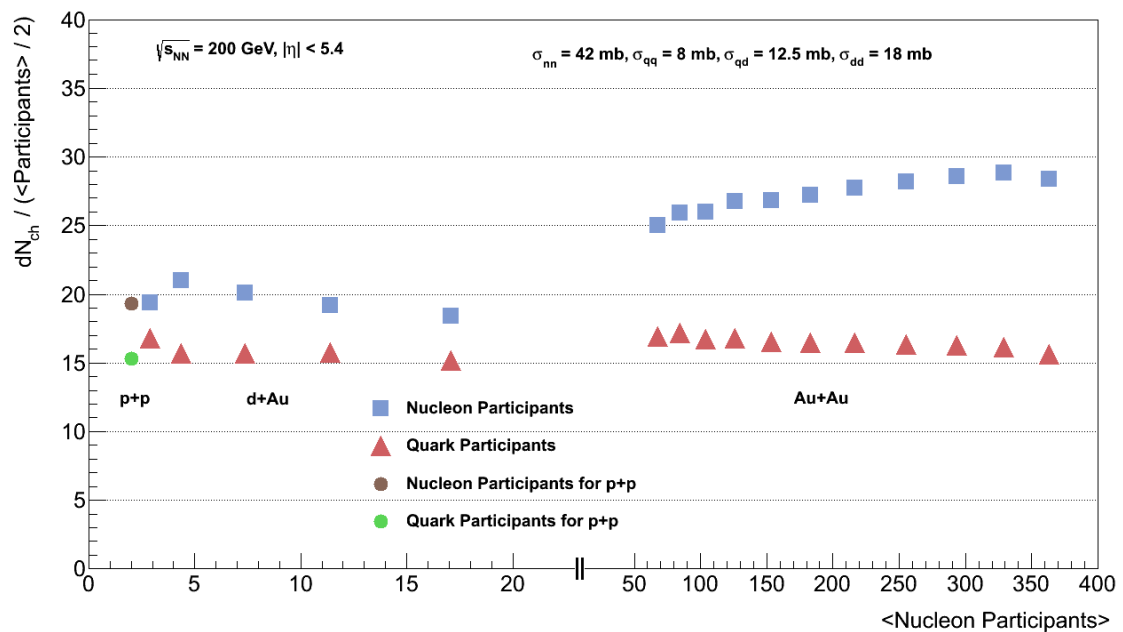
Figure 23: The ratio of total charged multiplicity dN_{ch} ($|\eta| < 5.4$) to the number of nucleon participant pairs $\langle N_{\mathrm{part}} \rangle / 2$ (at the top) and quark participant pairs $\langle Q_{\mathrm{part}} \rangle / 2$ (at the bottom) are plotted at a center-of-mass energy of $\sqrt{s_{\mathrm{NN}}} = 200\,\mathrm{GeV}$ for p+p, d+Au and Au+Au collisions versus the nucleon participants N_{part}. The used cross sections are: $\sigma_{\mathrm{nn}} = 42\,\mathrm{mb}$, $\sigma_{\mathrm{qq}} = 8\,\mathrm{mb}$, $\sigma_{\mathrm{qd}} = 12.5\,\mathrm{mb}$, $\sigma_{\mathrm{dd}} = 18\,\mathrm{mb}$.

In Figure 23 we see that the multiplicity scales only approximately with the number of quark participants. Especially for peripheral Au+Au collisions the ratio of multiplicity to quark participant pairs is a little too large. However, we see

a consistency in the plotted data from p+p,d+Au to central Au+Au collisions.

The result looks quite similar as the one in the previous section, see Figure 22 and Figure 23. The difference between these two plots is that in the first one the cross sections for quark-quark, quark-diquark and diquark-diquark are identical whereas in the second one they are different.

When the cross sections are different it turns out that 25% of all quark-quark interactions have a cross section of $\sigma_{qq} = 8 \, \text{mb}$. 50% have a cross section of $\sigma_{qd} = 12.5 \, \text{mb}$. 25% of the quark-quark interactions have a cross section of $\sigma_{dd} = 18 \, \text{mb}$. On average we find: $0.25 \cdot 8 \, \text{mb} + 0.5 \cdot 12.5 \, \text{mb} + 0.25 \cdot 18 \, \text{mb} = 12.75 \, \text{mb}$. This is quite the same value as the cross section of $\sigma_{qq} = \sigma_{qd} = \sigma_{dd} = 12 \, \text{mb}$ we use for Figure 22. We conclude that differences between identical and different cross sections for quarks and diquarks are negligible. Hence, the results look similar.

Therefore we find again that the diquark constituent model approximately describes the total multiplicity in heavy-ion collisions.

6 Conclusions and Outlook

The results presented within this thesis demonstrate that the multiplicity production in Au+Au collisions at midrapidity ($|\eta| < 1$) and $\sqrt{s_{\mathrm{NN}}} = 200\,\mathrm{GeV}$ can be described by a constituent participant model with 3 quarks. The model fails in the description of data for very peripheral Au+Au collisions at midapidity ($|\eta| < 1$) as well as for Pb+Pb collisions at midrapidity ($|\eta| < 0.5$) and $\sqrt{s_{\mathrm{NN}}} = 2.76\,\mathrm{TeV}$. The model also fails in the description of the total charged multiplicity ($|\eta| < 5.4$) for Au+Au collisions at $\sqrt{s_{\mathrm{NN}}} = 200\,\mathrm{GeV}$. Furthermore it could be shown that there is no consistent description for the total charged multiplicity in p+p, d+Au and Au+Au collisions at $\sqrt{s_{\mathrm{NN}}} = 200\,\mathrm{GeV}$.

The total charged multiplicity production in Au+Au collisions ($|\eta| < 5.4$) and $\sqrt{s_{\mathrm{NN}}} = 200\,\mathrm{GeV}$ can be described by a diquark model. We have shown that for $\sigma_{\mathrm{qq}} = \sigma_{\mathrm{qd}} = \sigma_{\mathrm{dd}} = 12\,\mathrm{mb}$ and $\sigma_{\mathrm{qq}} = 8\,\mathrm{mb}$, $\sigma_{\mathrm{qd}} = 12.5\,\mathrm{mb}$, $\sigma_{\mathrm{dd}} = 18\,\mathrm{mb}$ there is a consistent description for the total charged multiplicity in p+p, d+Au and Au+Au collisions at $\sqrt{s_{\mathrm{NN}}} = 200\,\mathrm{GeV}$. In addition we have seen that it is irrelevant whether the quark-quark cross section is equal to the diquark-diquark cross section or not.

In the next step data for other energies and nuclei have to be analyzed. In addition the physical meaning of the free parameter σ_{qq} should be studied. Predictions could be made for multiplicities in p+Pb collisions soon to be measured at the LHC.

7 References

[A$^+$86]   R.E. Ansorge et al. Diffraction Dissociation at the Cern Pulsed Collider at cm Energies of 900-GeV and 200-GeV. *Z.Phys.*, C33:175, 1986.

[AAA$^+$05]   S.S. Adler, S. Afanasiev, C. Aidala, N.N. Ajitanand, Y. Akiba, J. Alexander, R. Amirikas, L. Aphecetche, S.H. Aronson, R. Averbeck, et al. Systematic studies of the centrality and $\sqrt{s_{NN}}$ dependence of the $dE_T/d\eta$ and $dN_{ch}/d\eta$ in heavy ion collisions at midrapidity. *Physical Review C*, 71(3):034908, 2005.

[APE$^+$93]   M. Anselmino, E. Predazzi, S. Ekelin, S. Fredriksson, and D.B. Lichtenberg. Diquarks. *Rev. Mod. Phys.*, 65:1199–1233, Oct 1993.

[Arm09]   N. Armesto. Predictions for the heavy-ion programme at the large hadron collider. *Arxiv preprint arXiv:0903.1330*, 2009.

[ASS78]   V.V. Anisovich, Y.M. Shabelsky, and V.M. Shekhter. Yields of projectile fragments in hadron-nucleus interactions and the quark structure of hadrons. *Nuclear Physics B*, 133(3):477 – 489, 1978.

[BCL82]   A. Bialas, W. Czyz, and L. Lesniak. Additive quark model of multiparticle production and nucleus-nucleus collisions at high energies. *Phys. Rev. D*, 25:2328–2340, May 1982.

[BHL$^+$80]   W. Busza, C. Halliwell, D. Luckey, P. Swartz, L. Votta, and C. Youngi. Experimental study of multiparticle production in hadron-nucleus interactions at high energy. *Physical Review D*, 22(1), 1980.

[Bia08]   A. Bialas. Wounded nucleons, wounded quarks: an update. *Journal of Physics G: Nuclear and Particle Physics*, 35:044053, 2008.

[Bia12]   A. Bialas. Wounded constituents. *Arxiv preprint arXiv:1202.4599*, 2012.

[Col11a]   ALICE Collaboration. Centrality dependence of the charged-particle multiplicity density at midrapidity in pb-pb collisions at $\sqrt{s_{NN}} = 2.76$ TeV. *Phys. Rev. Lett.*, 106:032301, Jan 2011.

[Col11b]   PHOBOS Collaboration. Charged-particle multiplicity and pseudorapidity distributions measured with the phobos detector in Au+Au, $Cu + Cu$, $d + Au$, and $p + p$ collisions at ultrarelativistic energies. *Phys. Rev. C*, 83:024913, Feb 2011.

[DVDJDV87] H. De Vries, C. W. De Jager, and C. De Vries. Nuclear charge-density-distribution parameters from elastic electron scattering. *Atomic data and nuclear data tables*, 36(3):495–536, 1987.

[EV03] S. Eremin and S. Voloshin. Nucleon participants or quark participants? *Physical Review C*, 67(6):64905, 2003.

[Flo10] W. Florkowski. Phenomenology of ultra-relativistic heavy-ion collisions. *World Scientific Pub Co Inc*, 2010.

[HL82] R.C. Hwa and C.S. Lam. Hadron wave functions and pion decay constant. *Phys. Rev. D*, 26:2338–2346, Nov 1982.

[KDW05] W. Kittel and E.A. De Wolf. Soft multihadron dynamics. *World Scientific Pub Co Inc*, 2005.

[MRSS07] M. L. Miller, K. Reygers, S. J. Sanders, and P. Steinberg. Glauber modeling in high energy nuclear collisions. *Ann.Rev.Nucl.Part.Sci.*, 57:205–243, 2007.

[PRSZ99] B. Povh, K. Rith, C. Scholz, and F. Zetsche. Teilchen und kerne, 5. edit. *Springer, Berlin*, 1999.

[RS11] K. Reygers and J. Stachel. Quark-Gluon Plasma Physics: from fixed target to LHC, lecture given at the University of Heidelberg. `http://www.physi.uni-heidelberg.de/~reygers/lectures/2011/qgp/qgp_lecture_ss2011.html,3.BasicsofNNandAACollisions`, 2011.

[Won94] C.Y. Wong. Introduction to high-energy heavy-ion collisions. *World Scientific Pub Co Inc*, 1994.

Acknowledgment

Declaration

I declare that I have written this thesis independently and that I have used no other than the specified sources and resources.

Heidelberg, July 16, 2012

....
Felix Frey